CONF-881045--3

LA-UR -88-1775

Received by OSTI

AUG 04 1988

LA-UR--88-1775

DE88 014472

TITLE: TELEVIEWER MEASUREMENT OF IN-SITU STRESS DIRECTION AT THE FENTON HILL HOT DRY ROCK SITE, NEW MEXICO

AUTHOR(S): Kerry Burns

SUBMITTED TO: Geothermal Resources Council
1988 Annual Meeting, 9-12 October 1988, San Diego
Transactions, Geothermal Resources Council

DISCLAIMER

DISCLAIMER

Portions of this document may be illegible in electronic image products. Images are produced from the best available original document.

TELEVIEWER MEASUREMENT OF THE ORIENTATION OF *IN SITU* STRESS AT THE FENTON HILL HOT DRY ROCK SITE, NEW MEXICO

Kerry L. Burns

Los Alamos National Laboratory

ABSTRACT

The *in situ* stress at Fenton Hill has been determined in drill hole EE-3A by observations of wellbore breakouts on imagery obtained with a televiewer logging tool. Wellbore shape, tool offcentering, and tool misalignment cause geometric distortions which have been treated by comparing imagery from two logging runs made six months apart. The comparison establishes that wellbore degradation in drill hole EE-3A is due to breakouts, which grow larger with time.

The azimuth of the axis of minimum horizontal principal stress is estimated to be 110.7 +/- 10.3 deg E of true N at a depth of 11,500 ft, increasing with depth at a rate of 1 deg per 50 ft. This method of measuring the orientation of horizontal principal axes is considerably more accurate than previous methods tried at Fenton Hill. The results agree generally with other stress indicators. The results support the concept that direction of reservoir growth during hydraulic stimulation favours the intermediate axis over other principal axes of stress.

I. INTRODUCTION

In situ stress is the natural state of stress at an operations site. It is the first state encountered in exploratory drilling, the state that persists in the farfield surrounding operating sites, and the state to which abandoned fields will eventually return.

The *in situ* stress is an important environmental parameter in the construction of artificial reservoirs for Hot Dry Rock geothermal energy. It controls which fractures will be activated and the amount of displacement that takes place on selected fractures. It thereby influences the geometry of the resultant network of inflated fractures and the permeability of any fluid pathway through the network.

At Fenton Hill, the *in situ* stress has been estimated by a variety of different tests and experiments. The methods fall into five groups, which are tectonophysical models, hydraulic models, seismic models, measurements on core, and measurements on the wellbore. Wellbore measurements include hydraulic fracturing and televiewer measurement of breakouts. The last is relatively new and offers promise of a satisfactory method for use in deep and hostile environments. This report describes the use of breakouts to measure *in situ* stress direction in drill hole EE-3A at the Hot Dry Rock site at Fenton Hill, New Mexico.

In this report, azimuth is written as deg E of MN or TN, where MN is magnetic north and TN is true. Magnetic north at Fenton Hill is 13 deg east of true north. It is convenient to name the principal stresses Sv, SH, and Sh, where Sv is approximately vertical, SH and Sh are approximately horizontal, and in terms of magnitudes, SH>=Sh. The symbol E-2 means divide by 100.

II. STRESS MEASUREMENT FROM WELLBORE FAILURES

A. Wellbore Failures

The stress distribution around a cylindrical opening in rock results from superposition of the *in situ* (far-field) stress and a cylindrically symmetric stress concentration around the opening (near-field or "hoop" stress). For reasons of physical symmetry, in the resultant field the conditions of failure are distinct and well-defined. The highest stresses occur on the boundary, at the wellbore-rock interface, so that any failure starts there and propagates into the rock, and the point of initiation is accessible to wellbore probes. The televiewer makes it possible to inspect wellbore failures and verify their cause, and from this to estimate the conditions of breakdown. Wellbore failures are therefore important indicators of rock properties and ground conditions.

B. Hydrofracturing Method

The first use of wellbore failure to measure *in situ* stress was hydraulic fracturing, where a fluid overpressure is applied inside the wellbore, and the resultant tensile splitting occurs in a direction that is oriented normal to the least principal stress. The hydrofracturing method has been widely applied. However, there has been increasing concern with the reliability of the method. Since wellbore breakdown can occur by other mechanisms, it is insufficient to apply the hydrofracturing model to all cases. This has spurred the development of televiewer technology as an inspection tool and widened the study of wellbore breakdown to include other mechanisms of failure.

B. Breakout Method

Breakouts are another type of wellbore failure. The spontaneous enlargement of cylindrical openings was first noted in the deep South African mines. It was recognized that the spalling was due to high compressive stress, with the broken-out segments causing wellbore elongation along the direction of minimum principal horizontal stress. It was then proposed that wellbore stability be determined from well records and used to estimate earth stresses and rock strength. This method is now an integral part of reservoir development in the petroleum industry.

The long axes of elongated boreholes, due to high, unequal, horizontal stresses, share common average orientation over considerable lengths of wellbore, or from wellbore to wellbore in a region. Regional consistency was demonstrated in the oilfields of Alberta and Texas, and it was concluded that the elongations can be used for regional surveys of crustal stress fields.

Representative recent televiewer studies of wellbore breakouts include Plumb and Hickman (1985) in Palaeozoic sediments of the New York Appalachians; Hickman, Healy and Zoback (1985) in the 1.6 km-deep Auburn geothermal well; Paillet and Kim (1987) in Cainozoic basalts of the Columbia Plateau in relation to nuclear waste disposal at the Hanford site; and by Guenot (1987) in relation to oil development in offshore Gabon, the Paris Basin, and the Meillon St. Faust field in SW France. These studies contain references to earlier work.

At the Fenton Hill Hot Dry Rock site, televiewer work was started by Burns (1987a,b,c) in wellbore GT-2. The discovery of breakouts in wellbore EE-3A led to studies by Barton et al. (1986, 1988), Barton and Zoback (1987), and Burns (1988).

C. Mechanics of Breakouts

Failure in compression occurs around circular openings regardless of size, and has been studied in shafts for uranium mining and nuclear waste disposal, and in tunnels for hydroelectric power development and underground military installations, as well as for wellbores. When the stresses around the opening exceed the rock mass strength, the rock yields and a "plastic" zone of nonelastic deformation develops (Fig. 1). Slip lines form around the boundary of the opening, as shown in Fig. 2, and make an angle of 45-f/2 deg with the maximum principal stress direction, where f is the angle of internal friction. The slip lines or fractures are initiated at the springline, the point of greatest stress concentration, and propagate into the rock. Breakouts are wedges of material freed between intersecting fractures. In a vertical wellbore, the breakouts form a line on the surface of the wellbore along the trace of the Sh-Sv stress plane. At any depth, the direction is the direction of Sh, the minimum horizontal principal stress. Laboratory tests and numerical simulations show that the failure starts with a lunate chip from the side of the wellbore and propagates outwards (Fig.3). Propagation occurs in discrete steps, with depth increasing, but width at the wellbore remains fairly constant.

Both field and laboratory studies support the idea that the breakouts originate by shear failure induced by stress concentrations in a biaxial stressfield; confirm that breakouts are oriented along the direction of minimum horizontal *in situ* stress; and establish that the widths of breakouts are related to the magnitude of *in situ* stress. Here we consider only stress direction, not magnitude.

III INTERPRETATION METHODS AND PROBLEMS

A. Pattern Recognition Problems

Televiewer log B was run in June 1985. The imagery was subjected to a sequence of operations designed to isolate the breakouts, resulting in the interpretation illustrated in Burns (1988). The breakouts are not invariably dark but may have central bright spots and brightened rims.

The problems of interpretation are discussed in detail in Burns (1978a,b,c; 1988). One difficulty is distinguishing breakouts from harmonic shading, where "harmonic shading" was the name given to an artifact caused in part by hole shape and tool off-centering. The breakouts identified in log B show some troubling attributes such as: (1) Only one end of many breakouts occurs on the imagery; (2) Where both ends occur, the angle between them is not always 180 deg and can be significantly less; and (3) There are sudden jumps in azimuth.

In order to study these anomalies, and confirm that the breakouts were properly identified, log B was digitized and the interpretations were verified against the software developed in the Borehole Geophysics Project at Stanford. The results (Barton et al, 1986, 1988) confirm the identifications of the breakouts, but fail to resolve all the geometric problems. A method of adjustment to compensate for eccentric hole shape and tool offcentering is described by Lysne (1986). However, the method assumes that the axis of the tool is aligned parallel to the axis of the wellbore. If tool is misaligned, the geometric problem cannot be solved from only one set of televiewer logs. This report describes the first attempt at adjustment based upon two different logs.

B. Matching Features

One way of separating artifacts from reality is to compare images made at different times. Real features should be repeated, artifacts not. Televiewer log B was run in drillhole EE-3A in June 1985. The survey was repeated in December to give log C. Logs B and C were two overlapping runs made six months apart. Breakouts did not occur in the same depth on each log, due in part to degradation of the wellbore between runs, and in part to lack of reproducibility in wireline depth between the two runs.

Images from logs B and C were compared for matching points. Examples of tie lines joining match points are shown in Fig. 4. Because the two ends of breakouts are never exactly 180 deg apart, it is necessary to distinguish between east-pointing and west-pointing ends. In Fig. 5, if A, B, C, ... are different viewpoints, we use Ea, Eb, Ec, ... for the azimuth of east-pointing ends, and Wa, Wb, Wc, ... for the west-pointing ends.

C. Measurement Results

The wireline depths of matching points in the two logs are compared in Fig. 6. The regular variation indicates that the points were well chosen.

The observed orientations are shown in Fig. 7. The circular mean azimuths and angular standard deviations are E = 100.26 +/- 12.58 for east-pointing breakouts (Eb and Ec), and W = 274.81 +/- 15.25 for west-pointing (Wb and Wc), in degrees E of MN. The difference W-E should be 180 deg but is 6 degrees less, a significant anomaly.

D. Azimuthal Distortion

The images were compared in pairs to find out whether the azimuths on one image agreed with the azimuths on another. Statistical summaries are in Table I.

Comparing logs B and C, we find the agreement is about 8 deg for east-pointing ends (103.75 - 096.07 = 7.62) and -7 deg for west-pointing ends (271.65 - 278.20 = -6.55).

On imagery from log B, the two ends of the breakouts are an average of 182.13 or 181.13 deg apart, that is, within 2 deg of being antiparallel. On imagery from log C, the difference angle is 167.76 or 167.90 deg, that is, about 12.1 deg away from antiparallel.

We conclude that there is a distortion in azimuth in both sets of logs, of different amounts. One effect is to change the angle between opposite ends of breakouts from 180 deg (which they should be) to about 12 deg less. Another effect is to change the azimuth of any end; for example, the east-pointing ends differ in azimuth by about 7 deg between logs B and C.

The "cross" or between-log discrepancy of 7 deg and the "auto" or within-log discrepancy of 12 deg are attributed to azimuthal distortion in the images. The amount of distortion must vary both within and between logs.

IV AZIMUTH ADJUSTMENT

A. Introduction

The anomalous azimuths are due to a combination of geometric factors, including tool offcentering and misalignment in a noncircular wellbore. Burns (1988) considered various combinations of these factors, and concluded that the major factors in this case are tool misalignment due to cable drag on the wellbore and entrainment of the tool centralizers in breakouts. These two factors predominate in borehole EE-3A; in other wells, different factors could be important.

B. Cable Drag

The direction of the lifting force is controlled, in this case, by the location of points of cable drag, as illustrated in Fig. 8. If the tool is free to rotate on the centralizing assembly, it will point along the cable direction, which is not the same direction as the wellbore axis at the tool. The effect is to tilt the tool with respect to the wellbore axis.

The direction of tilt can be determined from a wellbore survey. Fig. 9 shows the direction of tool displacement for that part of drillhole EE-3A between 11,300 and 11,900 ft depth, based on the wellbore survey of Schrader (1985). Tool off-centering in the interval is controlled by cable drag at 11,000 ft. The wellbore orientation is fairly constant, with a declination and inclination of about 130 deg E of MN and 82 deg below the horizon. The calculated directions of tool offcentering range from 309 deg at 11,300 ft to 009 deg E of MN at 11,900 ft.

C. Entrainment of Bowsprings

The angular bisector of the breakouts in logs B and C in Table I has mean values of 187.14 and 187.87 deg E of MN, respectively. The regressions against depth are almost coincident, being y = 185.43 + 2.45E-2(Z-11,500) for log B and y = 186.34 + 1.98E-2(Z-11,500). The difference at 11,500 ft is only 0.91 deg. These are so close as to imply that Ba and Ca (see Fig. 5) are not simply approximately parallel, but are constrained to be parallel. An explanation is that the bowsprings on the televiewer centralizing assembly have "keyed" into the breakouts, and whatever forces are applied to the tool, it is only free to tilt in one direction. It is concluded that the tool axis was displaced from the wellbore axis in almost the same direction on both runs. The concept leads to a "bisector" method of azimuth adjustment.

Details of the method are given in Burns (1988). The centering correction, expressed as an angle, averages about 1 deg for log B and 6 deg for log C. The tool locations implied by the adjustment are shown in Fig. 10. The tool was swinging freely about the center for log B, but was systematically tilted offcenter for log C. The direction of offcentering is not always consistent with the direction of cable drag shown in Figure 9, which means that the centralizers were distorted by forces applied to the centralizer arms by the sides of the breakouts. This explains the great difficulty in moving the tool through the hole on run C.

D. Adjusted Azimuths by the Bisector Method

Fig. 11 shows the centered azimuths of the breakouts after adjustment by the bisector method. The circular mean value and angular standard deviation are estimated at Ea = 097.66 +/- 10.31 deg E of MN for the east-pointing ends. The west pointing end can be found from Wa = Ea +180. The variation with depth is indicated by the regression line.

V SUPPORTING MEASUREMENTS

The best estimate of the minimum horizontal principal stress direction is 110.7 +/- 10.3 deg E of TN. Other estimates for EE-3A have been made using log C only. These are 106.1 +/- 16.3 deg E of TN, based on 1473 breakouts, (Barton et al., 1986); 104.9 +/- 10.9 based on 839 individuals (Barton and Zoback, 1987); and 106 +/- 11 based on 928 individuals (Barton et al., 1988). The estimate derived here, although based on many fewer individuals (99), is considered to be more accurate, as it is based on a geometrical reconstruction which depends upon information from two different logs B and C.

The estimated stress direction agrees with other data from Fenton Hill. The tectonophysical estimate of the least principal horizontal stress is, for example, is 100.5 deg E of TN (Burns, 1985).

The breakouts only give stress directions in the horizontal plane. From the tectonic setting, we identify the breakout direction (111 deg EofTN) as Sh, Sv is near-vertical, SH trends 021 deg EofTN, and the stresses are related by magnitude according to Sv>SH>Sh.

VI RESERVOIR IMPLICATIONS

The location of fluid pathways in the artificial reservoir at Fenton Hill is deduced from the location of microseismic events. The events occupy a roughly elliptical volume. If we use the terminology **Ra**, **Rb**, and **Rc** for the long, intermediate and short axes, respectively, of that volume, we find that approximately, **Ra=SH**, **Rb=Sv** and **Rc=Sh**. The intermediate principal axis of *in situ* stress (SH) is the most favoured direction of reservoir growth, while the least principal axis (Sh) is favoured least. The agreement in orientation is not exact, because other factors help determine reservoir shape, but the *in situ* stress is a prominent factor.

VII CONCLUSIONS

The wellbore breakout can be recognized by several diagnostic characters and gives a consistent indication of stress direction.

The degradation of the wellbore in the six months between logs B and C was substantial. The cause of the degradation reported by Dreesen et al (1986) is found, as a result of this work, to be almost entirely due to breakouts.

The "bisector" method of adjustment yields our final estimate, 110.7 +/- 10.3 deg. E of true N. This is the direction of the minimum horizontal principal stress.

REFERENCES

Barton, C. A., Zoback, M. D., 1987, Digital Borehole Televiewer Data Analysis: A Case Study. In Situ Stress Orientation at the Fenton Geothermal Site, New Mexico, Determined from Wellbore Breakouts: *Stanford Rock and Borehole Project*, v. 31, May 1987, pp. 253-278, Stanford University.

Barton, C. A., Zoback, M. D., Burns, K. L., 1988, In-Situ Stress Orientation and Magnitude at the Fenton Geothermal Site, New Mexico, Determined from Wellbore Breakouts: *Geophys. Res. Letters*, in press.

Barton, C. A., Zoback, M. D., Burns, K. L., Hess, A., Hodges, R., 1986, In-Situ Stress Orientation at the Fenton Geothermal Site, New Mexico, Determined from Wellbore Breakouts: AGU Fall Meeting, San Francisco, *EOS Trans. AGU.*, v. 67, n. 44, p.1206, abstr.

Burns, K., 1985, Reconstruction of the Stress Field at Fenton Hill: pp. 7-10 in Heiken G., compiler, *Workshop on Recent Research in the Valles Caldera, Los Alamos, N. M., October 15-18, 1984*; Report LA-10339-C, Los Alamos National Laboratory.

Burns, K. L., 1987a,b,c, *Geological Structures from Televiewer Logs of GT-2, Fenton Hill, New Mexico*: Part 1, Feature Extraction, July 1987, 40pp., Part 2, Rectification, August 1987, 40pp., Part 3, Quality Control, December 1987, 18pp., Report LA-10619-HDR, Los Alamos National Laboratory.

Burns, K. L., 1988, *Feature Extraction from Televiewer Logs of Inclined Drill Hole EE-3A, Fenton Hill. Lithology, Structure and Stress-Induced Breakouts in Granitic Gneiss*: Report, Los Alamos National Laboratory, in prep.

Dreesen, D. S., Dash, Z. V., Burns, K. L., Chavez, P., Kelkar, S., Kolar, J., Levy, S. S., 1986, Fracture detection: interpretation of well logs to select packer seats and locate injection intervals: *11th Annual Workshop on Geothermal Reservoir Engineering, Stanford University, California, January 21-23, 1986*.

Guenot, A., 1987, Borehole Breakouts and Stress Field: *Workshop on Fluid Flow through Fractured Rock, April 13-15, 1987, Garchy, France.*

Hickman, S. H., Healy, J. H., Zoback, M. D., 1985, In Situ Stress, Natural Fracture Distribution, and Borehole Elongation in the Auburn Geothermal Well, Auburn, New York: *J. Geophys. Res.*, v. 90, n. B7, pp. 5497-5512.

Labreche, D. A., Auld, H. E., 1980, *Analysis of Tunnel Linings for Deep Basing Structures*: Final Report, AFWL-TR-80-5, University of New Mexico, NM, September 1980.

Lysne, P., 1986, Determination of Borehole Shape by Inversion of Televiewer Data: *The Log Analyst*, May-June 1986, pp. 64-71.

Mastin, L. G., 1984, *Development of Borehole Breakouts in Sandstone*: M. S. thesis, Stanford University.

Paillet, F. L., Kim, K., 1987, Character and Distribution of Borehole Breakouts and Their Relationship to In Situ Stresses in Deep Columbia River Basalts: *J. Geophys. Res.*, v. 92, n. B7, pp. 6223-6234.

Plumb, R. A., Hickman, S. H., 1985, Stress-Induced Borehole Elongation: A Comparison Between the Four-Arm Dipmeter and the Borehole Televiewer in the Auburn Geothermal Well: *J. Geophys. Res.*, v. 90, n. B7, pp. 5513-5521.

Schrader, J., 1985, *Report of Sub-Surface Directional Survey. Los Alamos National Labs., Energy Extraction No. 3-A, Sandoval County, New Mexico*: Seeker Gyro Survey, Job No. RM685 A1586, 20 June 1985, Eastman Whipstock, Houston, Texas.

ACKNOWLEDGEMENT

This work performed under the auspices of the US Department of Energy.

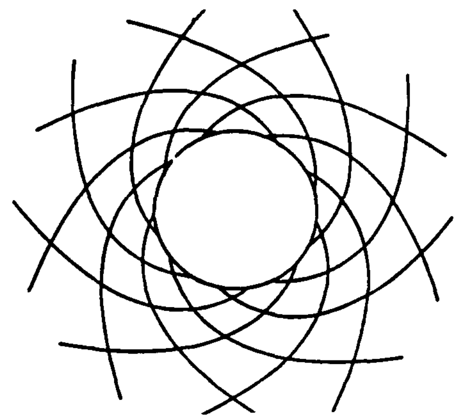

FIGURE 1: Plastic slip lines for Coulomb-Navier material in a hydrostatic stress field with an angle of internal friction of 35 deg. The figure shows the pattern of logarithmic spirals. After Labreche and Auld, 1980, Fig. 27.

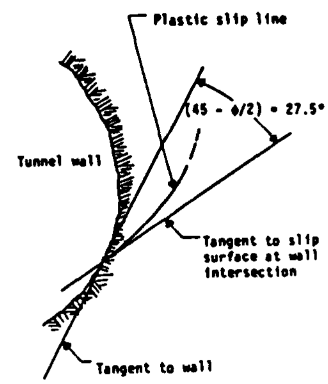

FIGURE 2: Angular relationships between the failure and wellbore surfaces at the springline. After Labreche and Auld, 1980, Fig. 27.

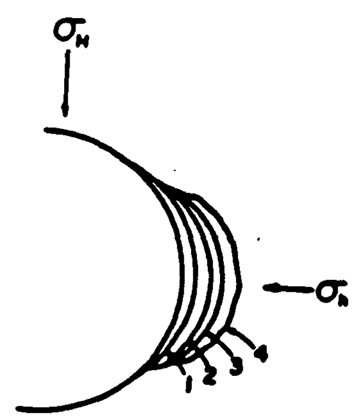

FIGURE 3: Size and shape of breakouts: numerical result of Mastin (1984) for a succession of failures.

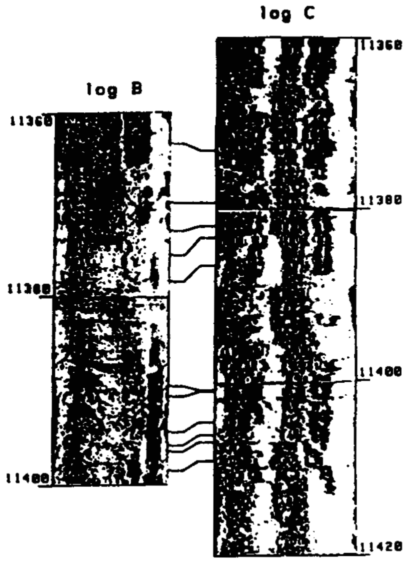

FIGURE 4: Example of reflected intensity logs. (left) log B, June, 1985; (right) log C, December 1985. The tie lines show the depths of matching features. New features appearing on the right image include new west-pointing breakouts from 11,380 to 11,388 ft, at 11,394 ft, from 11,399 to 11,408 ft, and an extension of an old west-pointing breakout from 11,411 to 11,414 ft. The dark stripes on the December image from 11,390 to 11,410 ft are west-pointing breakouts. On the June image they are absent, and the west-pointing effect is harmonic shading. Drillhole EE-3A, Fenton Hill, magnetic azimuth 0 to 360, from left to right; overlap depth 11,360 to 11,400 ft, from top to bottom.

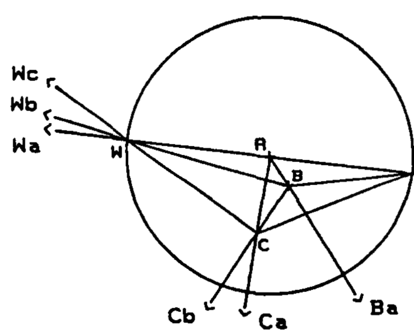

FIGURE 5: Azimuth terminology. Point A is at the center of the circular wellbore. Points B and C are off-centered tool positions, bearing at Ba and Ca from A. The point C bears at Cb from B. Points E and W are the east- and west-pointing ends of a breakout. For a tool centered at A in the wellbore, the ends of the breakout at E and W have azimuths of Ea and Wa, as seen from the tool, which are 180 deg apart. When the tool is shifted to locations B or C, the azimuths change to Eb and Wb, Ec and Wc, which are no longer 180 deg apart. Similar effects are caused by misalignment of tool and wellbore axis.

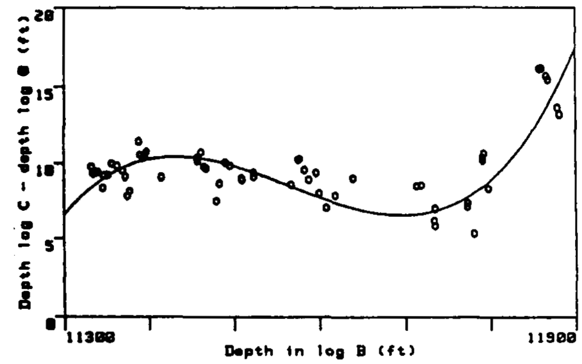

FIGURE 6: Matching points in two logs. The features matched were breakouts, as seen at different times, on logging runs B and C. The relationship plotted is Dz (depth in log C - depth in log B) versus Z (depth in log B), for 63 matching features. The solid line is the cubic regression. The linear mean +/- standard deviation is Dz = 9.34 +/- 2.84 ft.

TABLE I: Pair-wise comparisons of the azimuths of matching points of breakouts. The columns refer to two different sets of televiewer logs, namely logs B and C. The breakouts have two ends, differentiated by the columns headed E and W. The data set "B vs C" refers to distinctive points of breakouts on log B that could also be identified on log C, and others similarly. The letter symbols on the rows are: i = identification of the data sets; n = number of breakouts found to match; r = concentration (0<=r<=1); m = circular mean azimuth in deg EofMN; s = angular standard deviation in deg; d = difference in mean azimuths between the two ends of the same breakout in deg, b = angular bisector of the mean azimuths of the east- and west-pointing breakouts in deg EofMN.

	Log B		Log C	
row	E	W	E	W
i	B vs B		B vs C	
n	49	61	49	61
r	0.9685	0.9544	0.9685	0.9544
m	096.07	278.20	096.07	278.20
1 s	14.49	17.51	14.49	17.51
d	182.13		181.13	
b	187.14		187.14	
i	C vs B		C vs C	
n	49	61	54	66
r	0.9868	0.9765	0.9876	0.9781
m	103.75	271.65	103.99	271.75
2 s	9.34	12.49	9.07	12.05
d	167.90		167.76	
b	187.70		187.87	
col	1e	1w	2e	2w

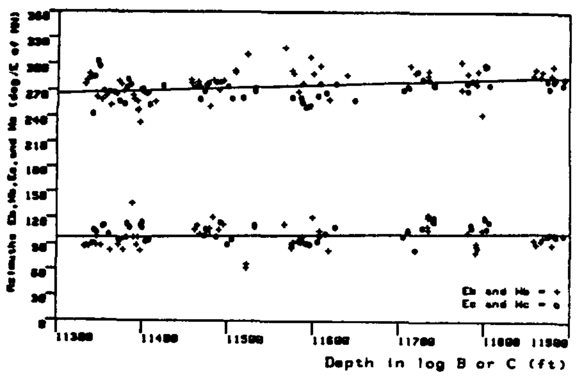

FIGURE 7: Observed azimuths of breakouts. The azimuths Eb, Wb, Ec and Wc were observed in reflected intensity logs B and C, and are plotted against their nominal depths in those logs. The solid lines are the linear regressions E = 099.27 + 1.22E-2(Z-11,500); and W = 272.51 + 3.16E-2(Z-11,500).

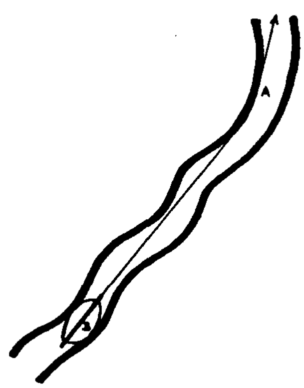

FIGURE 8: Cable drag acting on a televiewer logging tool.

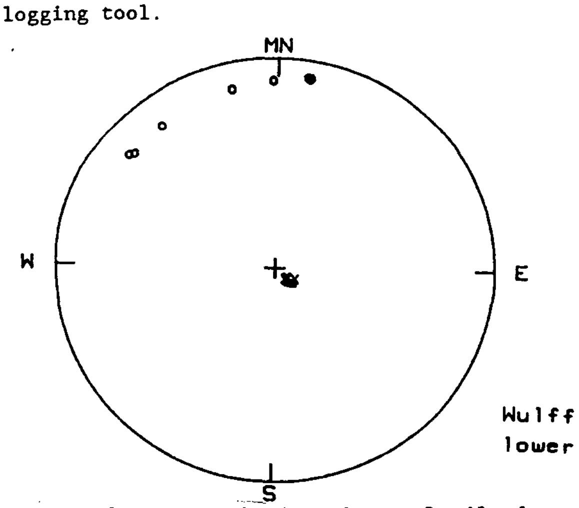

FIGURE 9: Expected directions of tilt between 11,200 and 11,900 ft, assuming the cable is dragging near 11,000 ft. Based on the geometry illustrated in Fig. 8 and the wellbore survey of drill hole EE-3A.

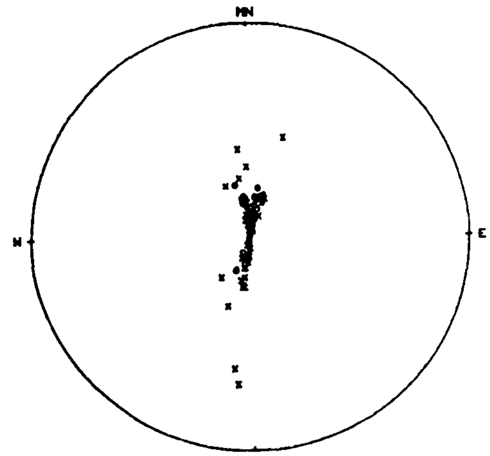

FIGURE 10: Locations of the logging tool in the wellbore. The diagram is a cross-section of a circular wellbore of radius 9.63 inches, showing the calculated location of the logging tool in the depth range 11,300 to 11,900 ft.

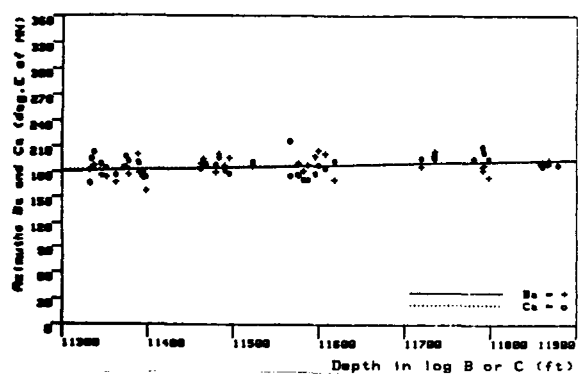

FIGURE 11: Azimuth of breakouts, adjusted by the bisector method. The azimuths for a centered tool, Ea and Wa, were calculated from the azimuths observed by off-centered tools, Eb, Wb, Ec, Wc as shown in Fig. 5, using the bisector method of adjustment. The depth is the nominal depth of the feature where it occurs in logs B and C. The solid lines are the linear regressions Ea = 095.88 + 2.21E-2(Z-11,500); and Wa = Ea + 180 where Z is depth in log B or log C. The trend is for azimuth to increase with depth.